Geophysical Corner

Bandwidth Extension of Seismic Data, Impact on Seismic Attribute Computation

Bandwidth extension of seismic data is a desirable goal when the available data has inadequate frequency content. Though significant efforts are expended during processing of seismic data to preserve the frequency content, they may not be effective enough to resolve reservoir intervals below tuning. We describe the performance of the sparse-layer seismic reflectivity inversion to extend the seismic bandwidth. This method yields a reflectivity series, which can be subsequently filtered to a desirable bandwidth that provides optimum resolution. These broader band results give reasonably accurate synthetic ties to wells and can also be used to derive relative acoustic impedance. By tightening the seismic wavelet and enhancing lateral changes in phase, bandwidth extension also improves lateral resolution as measured by volumetric dip, coherence, and curvature attributes.

Given these improvements, we apply two different unsupervised machine learning methods to attributes computed from the bandwidth extended data and compare them to the results computed from the original data. We find bandwidth extension provides a higher level of detail, whether it is the lineaments corresponding to faults or the thin-layered lithointervals than classification of the original data.

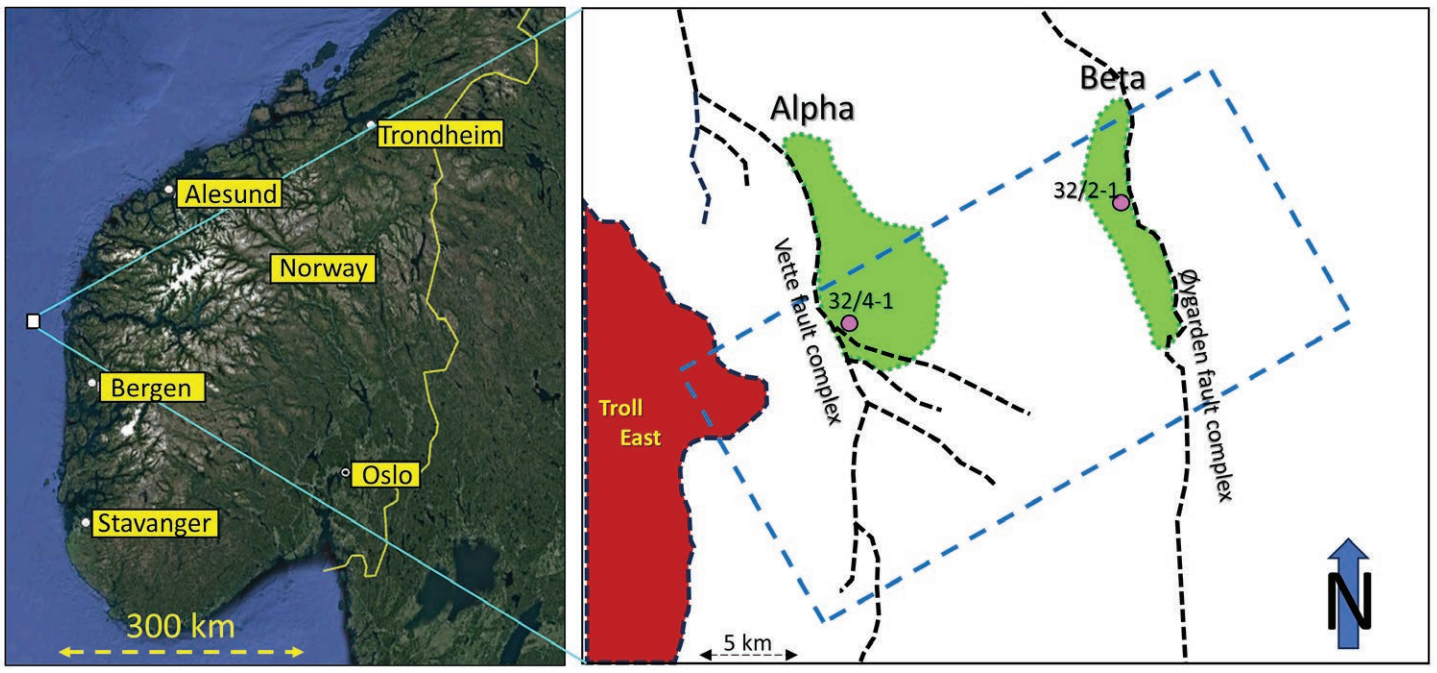

Figure 1: (Left) Location of the Smeaheia area on the Norwegian continental shelf. (Right) Zoom of the Smeaheia area indicating the two interpreted structures, 'Alpha' and 'Beta.' The two main fault complexes in the area are marked as dashed black lines. The dashed blue rectangle depicts the outline of the 3-D seismic volume being used, and the dashed red line is the location of the seismic inline segments shown in figures 4 and 7. The image to the left was prepared with the use of Google Earth Pro. (Modified after Furre et al., 2017.)

Sparse-Layer Seismic Reflectivity Inversion

In the sparse-layer seismic reflectivity inversion method a temporally and spatially varying wavelet estimate is used. Just as an isolated spike (with an unknown wavelet) forms the basis function in spiking deconvolution, a library of thin-bed responses comprising dipole (two-layer or thin-bed) basis functions (layer responses) are convolved with the wavelet field using a priori information and statistical assumptions. The basis functions are then fit to the data using a least-squares fit criterion. The sparse-layer inversion determines a sparse number of patterns which, when summed together, form the original seismic trace. To extend the bandwidth, we now use the same dipoles that were convolved with the original wavelet field, but now replace the original wavelet with one with an extended bandwidth. Explicitly stated, the algorithm replaces the original data with a model of dipoles convolved with the well-log generated synthetic wavelet or statistical wavelet with a wavelet of our own choosing. In this manner, the unmeasured high and low frequencies in the new extended bandwidth wavelet are consistent with the same model used to represent the original data.

The sparse-layer inversion does not directly use well data in the inversion, though well data may be used in wavelet extraction and parameter selection (such as degree of sparsity), and of course for validation. By operating on a trace-by-trace basis, this inversion yields a reflectivity series, which is then filtered to a desirable bandwidth that exhibits an optimum combination of resolution and reasonably accurate synthetic ties to wells. The output

Continued on next page ▶

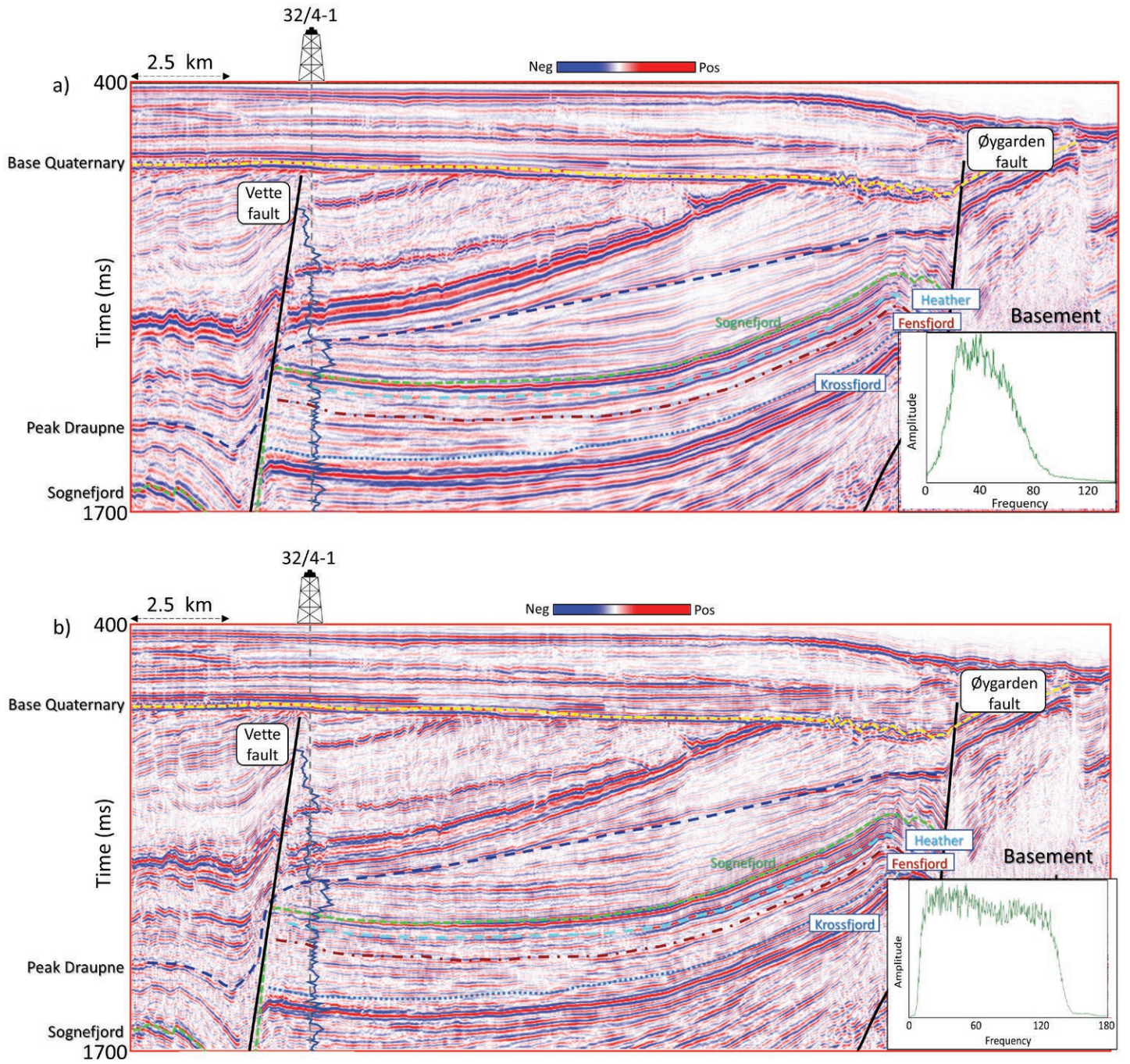

Figure 3: Segment of an inline extracted from (a) input seismic data volume, and (b) input seismic data volume after bandwidth extension. Some relevant markers and gamma ray curve for well 32/4-1 are overlaid on the two sections. The frequency spectra (computed over the time window exhibited and over the whole seismic volume) for the two data volumes are also shown to the right. Notice the enhancement in the resolution of the reflections after bandwidth extension. Notice, the low and higher frequencies after bandwidth extension contribute to the higher resolution.

◀ Continued from previous page

reflectivity series can also be used to derive relative acoustic impedance.

We use the 3-D seismic data from Smeaheia area in offshore Norway to demonstrate the value of sparse layer inversion, where the Smeaheia area is a candidate for CO_2 storage and evaluation.

The Smeahiea area lies about 30 kilometers east of the Troll gas field (figure 1), within the Norwegian continental shelf. It is located in a fault block bounded by the Vette Fault to the west and the Øygarden Fault to the east and is raised about 300 meters relative to the Troll field. The Late Jurassic Sognefjord, Fensfjord and Krossfjord formations form the producing reservoir zones in the Troll gas field.

In the Smeaheia block, there are two four-way closure structures, the Alpha structure to the west and the Beta structure to the east. Two exploration wells, namely 32/4-1 and 32/2-1 have been drilled into these structures, and although the reservoir is good, both wells turned out to be dry, indicating that the Smeaheia area is not charged with hydrocarbons.

In the Smeaheia area, the Sognefjord Formation is the primary reservoir consisting of medium to coarse-grain, well-sorted, micaceous and minor argillaceous sandstone. Below this formation lies the Fensfjord Formation consisting of medium-grained, well-sorted sandstone with shale intercalations. Underlying the Fensfjord Formation is the Krossfjord Formation with medium to coarse-grained, well-sorted sandstone.

Overlying the Sognefjord Formation are the Heather and Draupne formation shales. While the Heather formation comprised of silty claystone with thin streaks of limestone interfingering the Sognefjord, Fensfjord and Krossfjord sandstones. The Draupne Formation consists of dark grey to brown/black shale that is non-calcareous, carbonaceous and fissile claystone. Both the Heather and Draupne formations serve as primary seals for the proposed CO_2 storage reservoir sandstones of the Sognefjord, Fensfjord and Krossfjord formations.

As the Sognefjord, Fensfjord and Krossfjord are sandstone reservoir formations, there is concern about evaluation of their properties for thicknesses that fall below seismic resolution, which could come from shale and carbonate stringers within these zones. Finally, the existence of faults/fractures that fall below seismic resolution could provide pathways for fluid losses. All these risks need to be evaluated and mitigated in the context of long-term CO_2 storage.

Available Data for Demonstration of Bandwidth Extension

The available seismic data were the GN1101 3-D survey covering the Smeaheia (blue dashed rectangle shown in figure 1) acquired by Gassnova in 2011 made publicly available by Gassnova and Equinor. The bin size for the data is 12.5 x 25 meters with a sample interval of 4 milliseconds. Gassnova provided interpreted horizons and well log data for the two 32/4-1 and 32/2-1 wells along with well completion reports. These logs consisted of the complete gamma ray curves, but the sonic and density logs were not recorded for the shallower depths. The seismic data volume is of good quality.

Figure 2 shows the correlation of well curves with seismic data. The blue traces represent the synthetic seismograms generated with the zero-phase wavelet shown above. The red traces represent the seismic data (a) before, and (b) after bandwidth extension. Windows of seismic data before and after bandwidth extension from where the red traces are extracted are also shown alongside. There is a reasonably good correlation between the synthetic and red traces in the time window for the bandwidth extended data; furthermore, there are more reflection cycles.

Figure 3a shows a segment of an inline seismic section extracted from the available seismic data volume (which has a bandpass filter applied), which passes through well 32/4-1 and exhibits the different markers overlaid. The gamma ray curve for well 32/4-1 is shown overlaid on the section. The 'Base Quaternary' (in yellow) represents an angular unconformity and the 'Peak Draupne' (in dark blue) the top of the shale formation. The 'Sognefjord' (in green), 'Fensfjord (in cyan) and 'Krossfjord' (in bluish green) are the markers of interest representing sandstone formations as described above. Two prominent faults in solid black (Vette fault to the west and Øygarden fault to the east) are also shown overlaid on the section. The frequency spectrum computed for the time interval of the seismic data exhibited is shown to the right, which indicates a roll-off of the frequencies beyond 40 hertz. The bandwidth extension method employed here uses the spectrum ranging from 5-80 hertz to define a model (the weights in the

See **GeoCorner** page ?? ▶

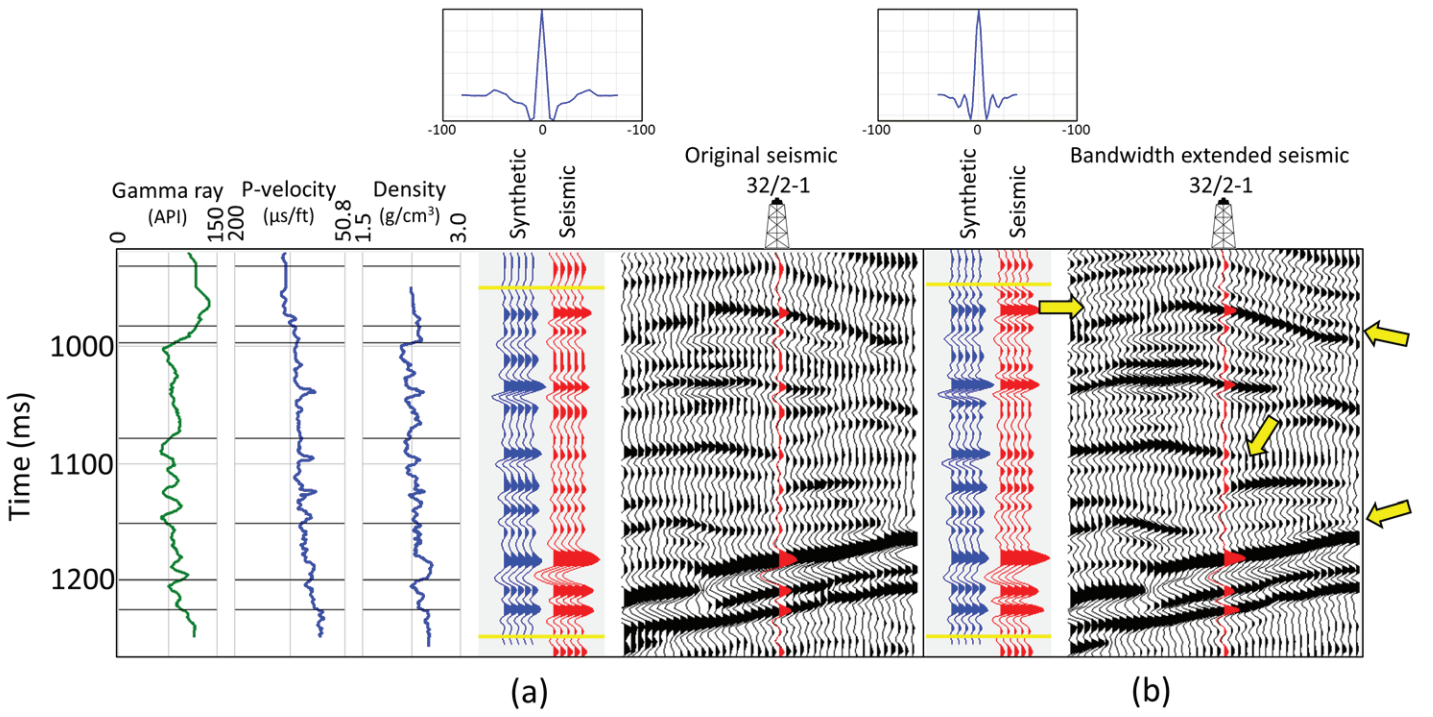

Figure 2: Correlation of well curves with seismic data. The blue traces represent the synthetics (generated with the wavelet shown above), whereas the red traces represent the seismic data (a) before, and (b) after bandwidth extension. The correlation coefficients for the ties were 0.745 for (a) and 0.756 for (b). Thus, there is a good correlation between the synthetic and red traces in the time window indicated for both data volumes but note the resolution of additional events after bandwidth extension indicated by the yellow arrows.

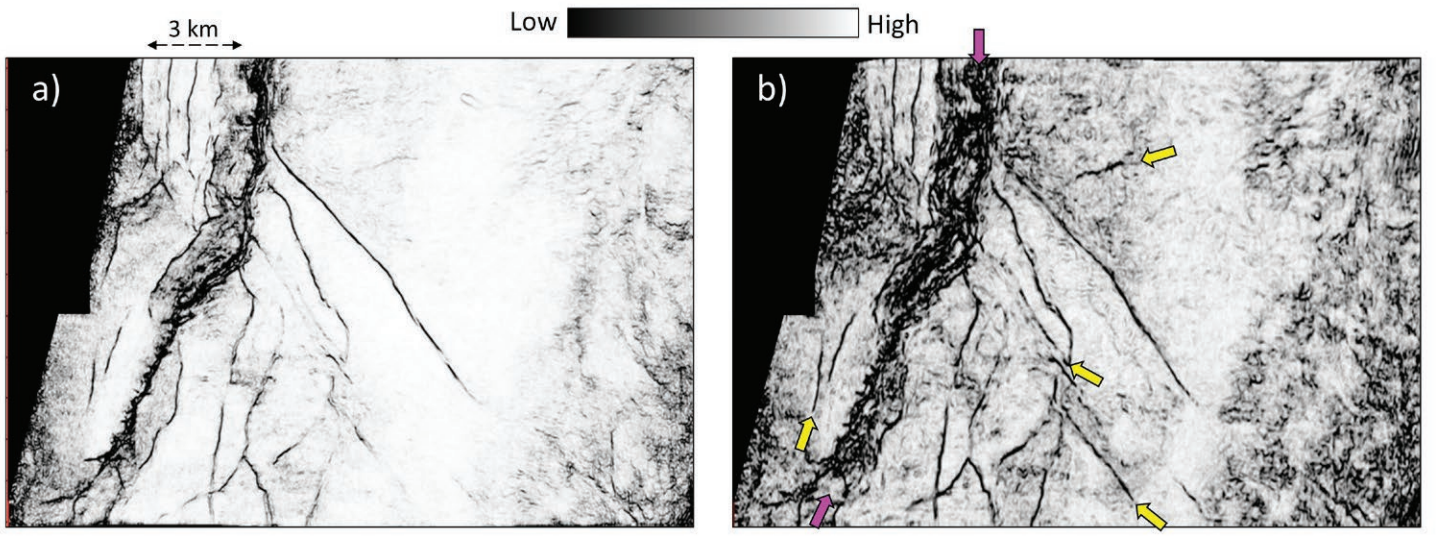

Figure 4: Time slice at 1.66 seconds through multispectral energy ratio coherence volumes computed on (a) input seismic data with structure-oriented filtering, and (b) input seismic data with bandwidth extension and structure-oriented filtering. Notice the superior definition of the lineaments in terms of their continuity and intensity seen on the display in (b). Some of the weak lineaments seen in (a) are better delineated in (b) indicated by yellow arrows. The fault damage zone indicated by magenta arrows is better defined in (b).

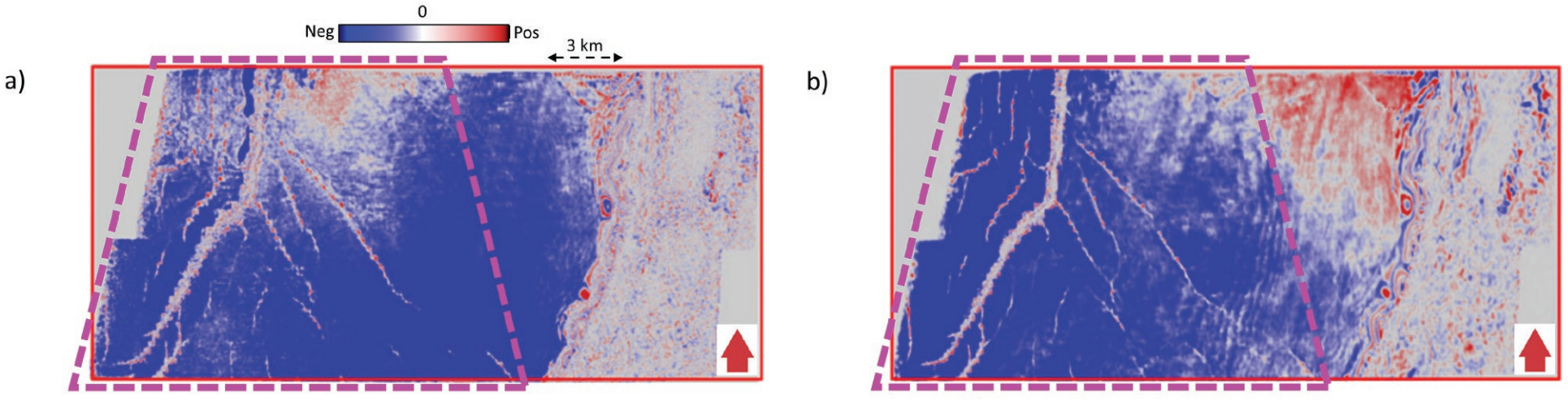

Figure 5: Stratal slice 32 milliseconds above the Sognefjord marker from the relative acoustic impedance attributes computed from (a) input seismic data, and (b) input seismic data after bandwidth extension. Notice the crisp definition of the faults highlighted areas in dashed purple outline in (b).

GeoCorner

from page ??

fit are the spectral magnitudes in figure 3a, so the 40 hertz is weighted more than 80 hertz). After 80 hertz the model extends the spectrum from 80 to 140 hertz where no data were measured.

Generation of Different Attributes

With the improved vertical resolution seen in figure 3b, our next task is to determine if bandwidth extension also enhances the lateral resolution as measured by seismic attributes such as coherence and curvature. Specifically, we anticipate that some lateral discontinuities fall near the limits of seismic resolution in the original data but will be better resolved in the bandwidth extension data.

- Energy ratio coherence: Encouraged with the higher-frequency content of the seismic data, we first generated the coherence attribute. Much has been written about this attribute and the usefulness of its application. We make use of the multispectral energy ratio-based coherence algorithm for which more details can be found in the July 2018 installment of Geophysical Corner.

Figure 4 shows a comparison of time slices at 1.66 seconds extracted from multispectral energy ratio coherence computed on the input seismic data with structure-oriented filtering (figure 4a) and input seismic data with bandwidth extension and structure-oriented filtering (figure 4b). Notice the superior definition of the lineaments in terms of their continuity and intensity seen on the display in figure 4b. Some of the weak lineaments seen in figure 4a appear nice and bright in figure 4b. The fault damage zone to the left is also much better defined in figure 4b.

Similarly, we generated the multispectral curvature attribute (more details can be found in the November and December 2007 installments of Geophysical Corner) and noticed superior definition of the lineaments in terms of their continuity, intensity and resolution seen on the displays (not shown here).

- Relative acoustic impedance is computed by continuous integration of the original seismic trace with the subsequent application of a low-cut filter. Because it assumes a zero-phase wavelet that is as close to a spike as possible, the improved resolution of bandwidth extension will provide improved results over the original data. The impedance transformation of seismic amplitudes enables the transition from reflection interface to interval properties of the data, without the requirement of a low-frequency model. A comparison of stratal slices 32 milliseconds above the Sognefjord marker from the relative acoustic impedance attributes computed from input seismic data and input seismic data after bandwidth extension is shown in figure 5. Notice the crisp definition of the faults as indicated by the highlighted areas in dashed purple outlines.

Likewise, the other attributes computed on the two seismic volumes are listed below along with their brief descriptions.

- Instantaneous envelope/frequency: Instantaneous envelope is a measure of the instantaneous energy of the analytic seismic trace, independent of phase, and provides information on intensity of reflections. Similarly, instantaneous frequency provides information on attenuation and layer thickness. We use a smoother, more stable version of the instantaneous frequency usually obtained by weighting it by the envelope.
- Sweetness: This is a "meta-attribute" or one computed from others, which in this case is the ratio of the envelope to the square root of the instantaneous frequency. A clean sand embedded in a shale will exhibit high envelope and lower instantaneous frequency, and thus higher sweetness, than the surrounding shale-on-shale reflections.
- GLCM energy: grey-level co-occurrence matrix energy is a measure of textural uniformity in the data. If the reflectivity along a horizon is nearly constant, it will exhibit high GLCM energy.
- Spectral magnitude: The magnitude of spectral components ranging from 20 to 70 hertz, which is the effective bandwidth of the input seismic data.

Specifically, the attributes used for the computation of seismic facies classification using some of the unsupervised machine learning methods were the relative acoustic impedance, envelope, sweetness, GLCM energy and spectral magnitudes at 25, 40 and 55 hertz.

All these different attributes have been generated on both the input seismic and the bandwidth extended versions to use them as input for unsupervised seismic facies classification using machine learning techniques, which are described in the next section.

Machine Learning Methods of Seismic Facies Classification

We apply two different unsupervised seismic facies classification machine learning methods, namely self-organizing mapping and generative topographic mapping, to them. A comparison of the two versions reveals supervisor spatial facies resolution as well as crisp definition of faults/fractures as seen on the bandwidth extended seismic data.

The description of both these methods can be found in our previously published articles in the January and November 2022 installments of Geophysical Corner.

- Self-organizing mapping: SOM is an unsupervised machine learning technique based on the clustering approach that generates a seismic facies map from multiple seismic attributes. In this technique the initial cluster centroids are defined in an N-dimensional attribute data space by fitting a plane defined by the first two eigen vectors of the covariance matrix to the data in a least-squares sense. With centroid still locked to this plane, it is iteratively deformed into a 2-D surface that fits the data still better. Once convergence is reached, the N-dimensional data are projected onto this 2-D surface. Thus,

Continued on next page ▶

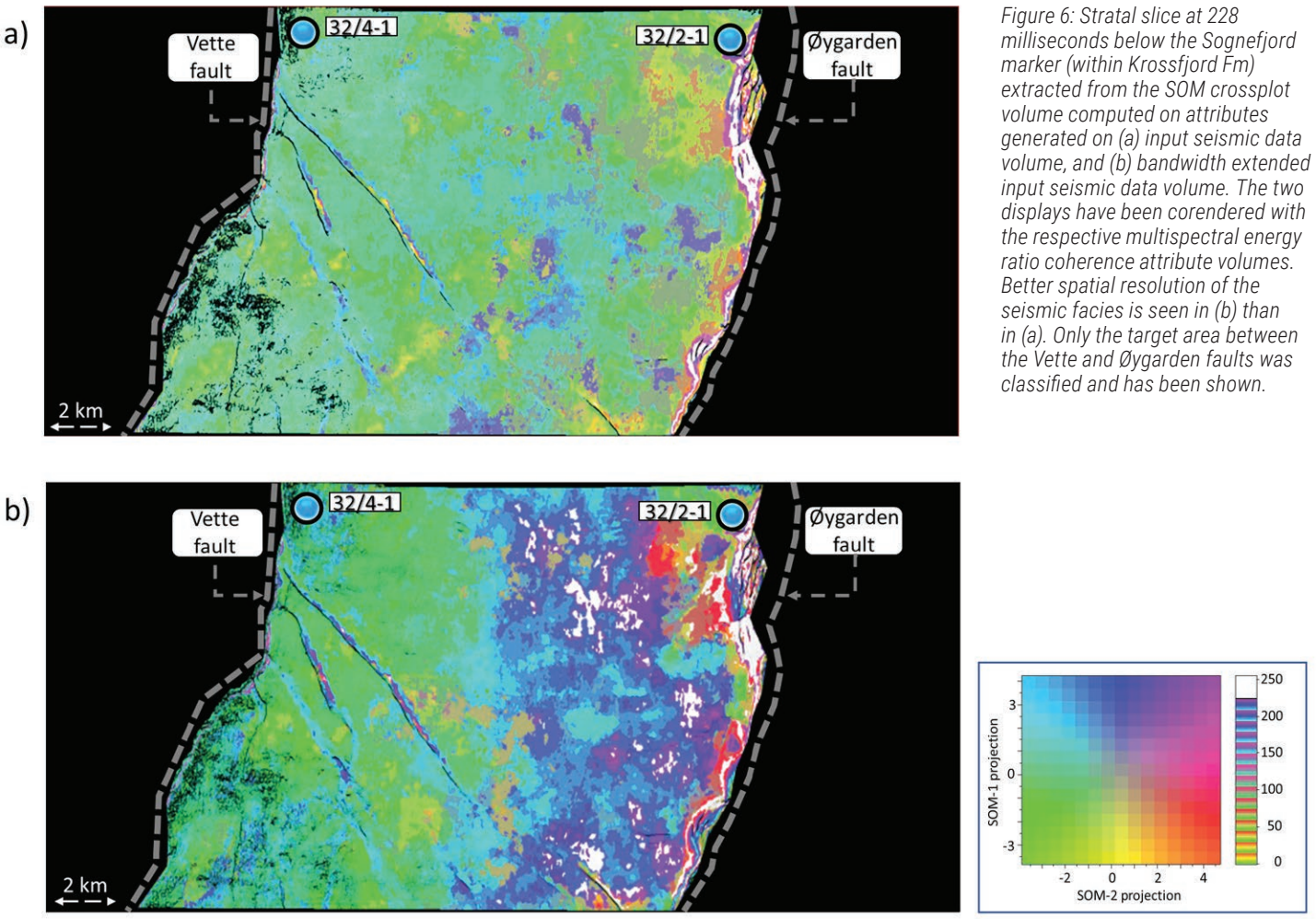

Figure 6: Stratal slice at 228 milliseconds below the Sognefjord marker (within Krossfjord Fm) extracted from the SOM crossplot volume computed on attributes generated on (a) input seismic data volume, and (b) bandwidth extended input seismic data volume. The two displays have been corendered with the respective multispectral energy ratio coherence attribute volumes. Better spatial resolution of the seismic facies is seen in (b) than in (a). Only the target area between the Vette and Øygarden faults was classified and has been shown.

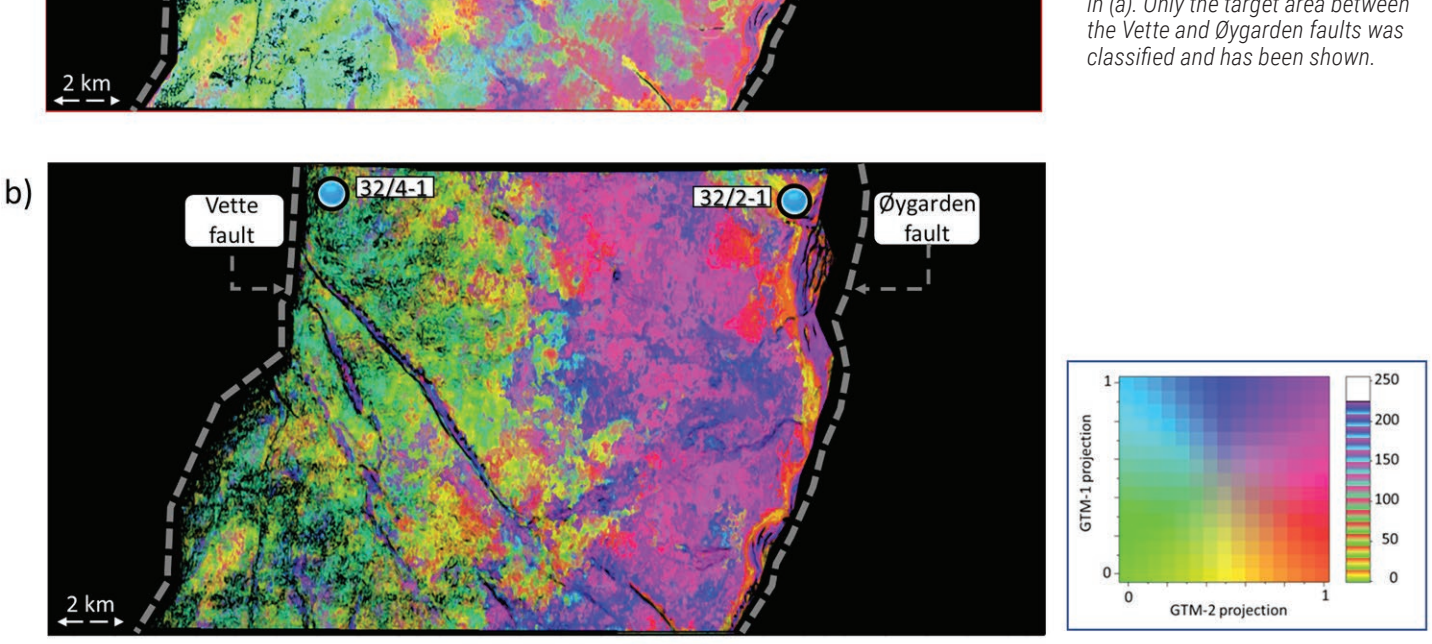

Figure 7: Stratal slice at 228 milliseconds below the Sognefjord marker (within Krossfjord Fm) extracted from the GTM crossplot volume computed on attributes generated on (a) input seismic data volume, and (b) bandwidth extended input seismic data volume. The two displays have been corendered with the respective multispectral energy ratio coherence attribute volumes. Better spatial resolution of the seismic facies is seen in (b) than in (a). Only the target area between the Vette and Øygarden faults was classified and has been shown.

Ritesh Kumar Sharma is with Calgary-based SamiGeo. He has vast experience of working with 2-D/3-D, land, and marine seismic data with different applications such as AVO analysis, rock-physics analysis, frequency enhancement of seismic data, simultaneous inversion, extended elastic impedance inversion as well as geostatistical inversion. He is an active member of SEG and CSEG.

John Castagna holds the Sheriff chair in geophysics at the University of Houston. His main research interest is the quantitative interpretation of seismic data.

Kurt Marfurt has divided his career nearly equally between industry and academia and is currently an emeritus professor of geophysics at the University of Oklahoma. For the past 20 years he has focused on seismic attributes and machine learning to aid the seismic interpreter. He has served as editor-in-chief for the SEG/AAPG journal Interpretation, has delivered two SEG distinguished instructor short courses, is the 2021-22 AAPG/SEG distinguished lecturer, and serves as an SEG director-at-large for 2020-22.

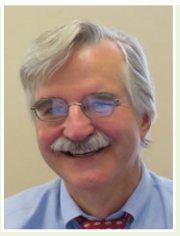

◀ Continued from previous page

SOM may be considered as projection from a multidimensional attribute space to a 2-D space or "latent" (hidden) space. Usually, the output from SOM computation is obtained in the form of two projections on the two SOM axes, which can then be directly crossplotted and displayed using a 2-D RGB color bar.

Figure 6 shows the equivalent stratal displays (within the Krossfjord formation) extracted from the SOM crossplot volume computed for the input and bandwidth extended versions of the seismic data, using a 2-D color bar. Some of the clusters seen on the display in figure 6b are better defined than the ones shown in figure 6a. Thus, a superior distribution of the seismic facies corresponding to the different colours for the SOM seismic facies generated on the bandwidth extended version is seen.

▶ Generative topographic mapping: Though the SOM method described above is easy to implement, is computationally inexpensive, and thus is a popular unsupervised clustering approach, it does have limitations. First, there is no theoretical basis for the selection of parameters such as training radius, neighborhood function and learning radius, as all of these are data dependent. Secondly, no cost function is defined in the method that could be iteratively minimized indicating convergence during the training process.

Finally, as a measure of confidence in the final clustering results, no probability density is defined. An alternative approach to the SOM method, called "generative topographic mapping," overcomes the above-stated limitations. It is a nonlinear dimension reduction technique that provides a probabilistic representation of the data vectors in latent space.

In figure 7 we show the displays equivalent to those shown for SOM analysis, where some of the clusters can be interpreted with ease with less background clutter and confusion.

Conclusions

We have found that bandwidth extension of the input seismic data improves not only the vertical resolution seen on vertical amplitude slices but also the lateral resolution of subsequent attributes computations displayed as time and horizon slices. Results obtained for the unsupervised machine learning applications employing both the input seismic as well as its bandwidth extended version depict superior performance of the latter in terms of clarity of clusters as well as color variations within them. Applications of SOM and GTM techniques to the same data allowed us to assess their relative strengths as well as their suitability. We found that GTM has an edge over SOM in terms of the detailed distribution of seismic facies in terms of better resolution and distinct definition of the geologic features seen on the displays.

Usually, the seismic facies maps in the zones of interest are calibrated with the lithofacies information obtained from well cores and cuttings. As there is appreciable difference in resolution between the two types of data, it is advisable to enhance the resolution of seismic data by adopting a bandwidth extension workflow. Such a workflow can narrow down the resolution gap between the facies data types (seismic and geologic) as well as help perform a better correlation/calibration between the two.

Though the analysis is qualitative at present, it paves the way for more detailed work as more well and production data become available.

Acknowledgements

The bandwidth extension work discussed in this paper employed the Ultra module owned by Lumina Technologies, Houston. The first author would also like to thank the Attribute-Assisted Seismic Processing and Interpretation (AASPI) Consortium, University of Oklahoma, for access to their software, which has been used for all attribute computation as well as subsurface AI (formerly Geomodeling Technology Corp.), Calgary, for making the Attribute-Studio software available. We wish to thank Gassnova and Equinor for access to the Smeaheia 3-D seismic and other associated data used in this exercise.

(Editors Note: The Geophysical Corner is a regular column in the EXPLORER, edited by Satinder Chopra, founder and president of SamiGeo, Calgary, Canada, and a past AAPG-SEG Joint Distinguished Lecturer.)